AD 14013

An Investigation of

THE EFFECTS OF STRESS CONCENTRATION AND TRIAXIALITY OF THE PLASTIC FLOW OF METALS

Technical Report No. 27
HYDROGEN EMBRITTLEMENT OF STEELS

By

Jack T. Brown
W. M. Baldwin, Jr.

Conducted By
METALS RESEARCH LABORATORY
DEPARTMENT OF METALLURGICAL ENGINEERING
CASE INSTITUTE OF TECHNOLOGY

In Cooperation With
OFFICE OF NAVAL RESEARCH, U. S. NAVY

Contract N6-onr-273/I Project NR-031-049

Cleveland, Ohio
June, 1953

METALS RESEARCH LABORATORY
DEPARTMENT OF METALLURGICAL ENGINEERING
CASE INSTITUTE OF TECHNOLOGY

Technical Report No. 27

HYDROGEN EMBRITTLEMENT OF STEELS

Written By:

Jack T. Brown

W. M. Baldwin, Jr.

Approved By:

L. J. Ebert
Assistant Task Order Director

W. M. Baldwin, Jr.
Task Order Director

Distribution List for
Technical Report
No. 27

Copy No. 16

Contract N6-onr-273/1 June, 1953 Project NR-031-049

Copy No.

1-2 Chief of Naval Research
Department of the Navy
Washington 25, D.C.
Attn: Code 423

3 Commanding Officer
Office of Naval Research
Branch Office
495 Summer Street
Boston 10, Massachusetts

4 Commanding Officer
Office of Naval Research
Branch Office
50 Church Street
New York 7, N. Y.

5 Commanding Officer
Office of Naval Research
Branch Office
John Crerar Library Bldg.
10th Floor, 86 E. Randolph St.
Chicago 11, Illinois

6 Commanding Officer
Office of Naval Research
Branch Office
801 Donahue Street
San Francisco 24, Calif.

7 Commanding Officer
Office of Naval Research
Branch Office
1030 Green Street
Pasadena, California

8 Assistant Naval Attache
for Research
London, England
U. S. Navy FPO #100
New York, N.Y.

9 Contract Administrator
SE Area, Office of Naval Res.
Department of the Navy
Washington 25, D. C.
Att: Mr. R. F. Lynch

10-18 Director, Naval Res. Lab.
Washington 25, D. C.
Att: Technical Information
Officer

19 Dr. C. S. Smith
Institute for the Study of Metal
University of Chicago
Chicago, Illinois

20-21 University of California
Engineering Department
Berkeley, California
Att: Dr. J. E. Dorn
Dr. E. R. Parker

22 Professor F. A. Biberstein
Department of Mech. Engr.
Catholic University of America
Washington, D. C.

23 Professor W. Prager
School of Applied Mathematics
Brown University
Providence, Rhode Island

24 Dr. L. V. Griffis
Applied Mechanics Division
Armour Research Foundation
Chicago, Illinois

25 Dr. W. C. MacGregor
Dept. of Mech. Engr.
Massachusetts Inst. of Tech.
Cambridge, Massachusetts

26 Director
David Taylor Model Basin
Washington 7, D. C.

27 Armour Research Foundation
Metals Research Division
35 W. 33rd Street
Chicago, Illinois
Att: W. E. Mahin

28-29 Director, Naval Res. Laboratory
Washington 25, D. C.
Attn: Code 2500, Metallurgy
Code 2020, Tech. Library

30-33 Bureau of Aeronautics
Department of the Navy
Washington 25, D. C.
Attn: N. E. Promisel, AE-41(3)
Technical Library, TD-41(1)

34 Commanding Officer
Naval Air Material Center
Naval Base Station
Philadelphia, Penna.
Attn: Aeronautical Materials
Laboratory

35-38 Bureau of Ordnance
Department of the Navy
Washington 25, D. C.
Attn: Rex (3)
Technical Library AD3(1)

39 Superintendent, Naval Gun Factory
Washington 20, D. C.
Attn: Metallurgical Lab IN910

40 Commanding Officer
U. S. Naval Ordnance Laboratory
White Oaks, Maryland

41 Commanding Officer
U. S. Naval Ordnance Test Station
Inyokern, California

42-45 Bureau of Ships
Department of the Navy
Washington 25, D. C.
Attn: Code 343 (3)
Code 337L, Tech. Lib. (1)

46 U. S. Naval Engineering Experiment
Station
Annapolis, Maryland
Attn: Metals Laboratory

47 Director, Materials Laboratory
Building 291
New York Naval Shipyard
Brooklyn 1, New York
Attn: Code 907

48 Bureau of Yards and Docks
Department of the Navy
Washington 25, D. C.
Attn: Research & Standards Div.

ARMY

49 Chief of Staff, U. S. Army
The Pentagon
Washington 25, D. C.
Attn: Director of Research &
Development

50-52 Office of Chief of Ordnance
Research & Development Service
Department of the Army
Washington 25, D. C.
Attn: ORDTB

53 Commanding Officer
Watertown Arsenal
Watertown, Massachusetts
Attn: Laboratory

54 Office of Chief of Engineers
Department of the Army
Washington 25, D. C.
Attn: Research & Development Br.

AIR FORCES

55 U. S. Air Forces
Research and Development Div.
The Pentagon
Washington 25, D. C.

56-57 Air Materiel Command
Wright-Patterson Air Force Base
Dayton, Ohio
Attn: Materials Laboratory MCREXM

OTHER GOVERNMENT AGENCIES

58 Atomic Energy Commission
Division of Research
Metallurgical Branch
Washington 25, D. C.

59 National Bureau of Standards
Washington 25, D. C.
Attn: Physical Metallurgy Division
Technical Library

60 National Advisory Committee
for Aeronautics
1724 F Street, N. W.
Washington 25, D. C.

61 Research & Development Board
Committee on Basic Physical
Sciences
The Pentagon
Washington 25, D. C
Attn: Metallurgy Panel

62 Commanding Officer
Naval Proving Grounds
Dahlgren, Virginia
Attn: Laboratory Division

63 Dr. Henry Eyring
School of Mines & Mineral Ind.
University of Utah
Salt Lake City, Utah

64 Dr. Finn Jonassen
National Research Council
2101 Constitution Avenue, N. W.
Washington 25, D. C.

65 Dr. E. P. Klier
Department of Metallurgy
University of Maryland
College Park, Md.

66 Dr. D. S. Clark
Department of Mech. Engr.
California Institute of Tech.
Pasadena, California

67-68 University of Illinois
Urbana, Illinois
Att: Dr. N. M. Newmark
Dr. T. J. Dolan

69 Dr. R. M. Brick
Department of Metallurgy
University of Pennsylvania
Philadelphia, Penna.

70 Bureau of Ships
Department of the Navy
Washington 25, D. C.
Attn: Code 692

71 Professor M. Cohen
Department of Metallurgy
Massachusetts Inst. of Tech.
Cambridge 39, Mass.

72 General Electric Company
Research Laboratories
Schenectady, New York
Attn: J. H. Hollomon

73 Dr. Robert Maddin
Department of Mech. Engr.
Johns Hopkins University
Baltimore, Maryland

74 Dr. R. F. Mehl
Director of Metals Research Lab.
Carnegie Institute of Tech.
Pittsburgh, Penna.

75 Brookhaven National Laboratory
Information & Publication Div.
Documents Section
Upton, New York
Attn: Miss Mary E. Waisman

76 Carbide and Carbon Chemicals Div.
Plant Records Department
Central Files (K-25)
P. O. Box P
Oak Ridge, Tennessee

77 Carbide and Carbon Chemicals Div.
Central Reports & Information
Office
P. O. Box P (Y-12)
Oak Ridge, Tennessee

78 General Electric Company
Technical Services Division
Technical Information Group
P. O. Box 100
Richland, Washington
Attn: Miss M. G. Freidank

79 Dr. M. Gensamer
Columbia University
New York, N. Y.

80 Iowa State College
P. O. Box 14A, Station A
Ames, Iowa
Attn: Dr. F. H. Spedding

81 Knolls Atomic Power Laboratory
P. O. Box 1072
Schenectady, New York
Attn: Document Librarian

82 Los Alamos Scientific Lab.
P. O. Box 1663
Los Alamos, New Mexico
Att: Document Custodian

83 U. S. Atomic Energy Commission
New York Operations Office
P. O. Box 30, Ansonia Station
New York 23, N. Y.
Attn: Division of Tech. Inf.
and Declassification Service

84 Oak Ridge National Laboratory
P. O. Box P
Oak Ridge, Tennessee
Attn: Central Files

85 Sandia Corporation
Sandia Base
Classified Document Division
Albuquerque, New Mexico
Attn: Mr. Dale N. Evans

86 U. S. Atomic Energy Commission
Library Branch, Tech. Inf.
Service, ORE
P. O. Box E
Oak Ridge, Tennessee

87 University of California
Radiation Laboratory
Information Division
Room 128, Building 50
Berkeley, California
Att: Dr. R. K. Wakerling

88 Westinghouse Electric Corp.
Atomic Power Division
P. O. Box 1468
Pittsburgh 30, Penna.
Attn: Librarian

89 Dr. W. M. Baldwin, Jr.
Case Institute of Technology

90 Professor K. H. Donaldson
Case Institute of Technology

91 Dean Elmer Hutchisson
Case Institute of Technology

92 Dr. A. R. Troiano
Case Institute of Technology

93 Mr. L. J. Ebert
Case Institute of Technology

94 Mr. E. J. Ripling
Case Institute of Technology

95 Mr. L. J. Klingler
Case Institute of Technology

96 Mr. Jack T. Brown
Case Institute of Technology

97 Metals Research Laboratory
Case Institute of Technology
(File Copy)

HYDROGEN EMBRITTLEMENT OF STEELS*

By

Jack T. Brown** and William M. Baldwin, Jr.***

ABSTRACT

The effect of hydrogen on the ductility, ε, of SAE 1020 steel at strain rates, $\dot{\varepsilon}$, from 0.05 inches per inch per minute to 19,000 inches per inch per minute and at temperature, T, from +150°F to -320°F was determined. The ductility surface of the embrittled steel reveals two domains: one in which

$$\left(\frac{\partial \varepsilon}{\partial \dot{\varepsilon}}\right)_T > 0, \quad \left(\frac{\partial \varepsilon}{\partial T}\right)_{\dot{\varepsilon}} < 0$$

and the other in which

$$\left(\frac{\partial \varepsilon}{\partial \dot{\varepsilon}}\right)_T > 0, \quad \left(\frac{\partial \varepsilon}{\partial T}\right)_{\dot{\varepsilon}} > 0$$

The usual "explanation" of hydrogen embrittlement are in accord with the first of these domains only.

- - - -

* This paper is based upon a portion of a research program conducted in the Metals Research Laboratory, Case Institute of Technology in cooperation with the Office of Naval Research. The data were used as the basis of a thesis submitted to Case Institute of Technology by Mr. Brown in partial fulfillment for the degree of Master of Science.

** Formerly graduate student, Case Institute of Technology, now at Westinghouse Research Laboratories, Pittsburgh, Pennsylvania

*** Research Professor, Metals Research Laboratory, Case Institute of Technology, Cleveland, Ohio.

INTRODUCTION

The purpose of this investigation was a fuller characterization of the effects of varying temperature and strain rate on the fracture strain of hydrogen charged steel.

To be sure, it is known that low and high temperature remove the embrittlement that hydrogen confers upon steels at room temperature (2) (10)(11)(12)*, see Fig. 1a and b, and that high strain rates have a similar effect (3)(4)(6)(12), see Figs. 2a, b, and c. However, the general effect of these two testing conditions on the fracture ductility of hydrogen-charged steels is not known, i.e., the three-dimensional graphical representation of fracture ductility as a function of temperature and strain rate is not known -- only two traverses of the graph are available. The need for such a graph is not pedantic. To demonstrate this point, Figs. 3a, b and c show three of many three-dimensional graphs, all possible on the basis of the two traverses at hand. The important point (as will be developed in the Discussion) is that each of them would indicate a different basic mechanism for hydrogen embrittlement.

It will be noted that the four types of ductility surfaces in Figs. 3a, b, and c may be characterized as follows:

Type "a": $\left(\frac{\partial \varepsilon}{\partial \dot{\varepsilon}}\right)_T > 0, \qquad \left(\frac{\partial \varepsilon}{\partial T}\right)_{\dot{\varepsilon}} < 0$

Type "b" $\left(\frac{\partial \varepsilon}{\partial \dot{\varepsilon}}\right)_T < 0, \qquad \left(\frac{\partial \varepsilon}{\partial T}\right)_{\dot{\varepsilon}} > 0$

Type "c" $\left(\frac{\partial \varepsilon}{\partial \dot{\varepsilon}}\right)_T < 0, \qquad \left(\frac{\partial \varepsilon}{\partial T}\right)_{\dot{\varepsilon}} < 0$

Type "d" $\left(\frac{\partial \varepsilon}{\partial \dot{\varepsilon}}\right)_T > 0, \qquad \left(\frac{\partial \varepsilon}{\partial T}\right)_{\dot{\varepsilon}} > 0$

---

* Numbers in parentheses pertain to references at the end of the paper.

MATERIAL AND PROCEDURE

Tensile tests were made at various temperatures and strain rates on a commercial grade of 3/4'' round SAE 1020 steel in both a virgin state and as charged with hydrogen. The steel was spheroidized at 1250°F for 168 hours to give the unembrittled steel the lowest possible transition temperature.

The steel was cathodically charged with hydrogen as follows: The specimen was attached to a six inch steel wire, degreased for five minutes in trichlorethylene, rinsed with water and fixed in a plastic top in the center of a cylindrical platinum mesh anode. The assembly was placed in a 1000 milliliter beaker containing an electrolyte of 900 milliliters of four per cent sulphuric acid and 10 milliliters of poison (2 grams of yellow phosphorous dissolved in 40 milliliters of carbon disulphide). A current density of one ampere per square inch was used which developed a four volt drop across the two electrodes. All electrolysis was carried on at room temperature.

Temperatures for tensile tests were obtained by immersing the specimens in baths of water (+70°F to +150°F), mixtures of liquid nitrogen and isopentane (+70°F to -240°F), and boiling nitrogen (-240°F to -320°F).

Specimens were tested in tension at strain rates of 0.05, 10, 100, 5000, 19000 inches per inch per minute. The 0.05 and 10 inches per inch per minute strain rates were obtained on a 10,000 pound Riehle Tensile Testing machine, the 100 inches per inch per minute rate on a hydraulic type draw bench with a special fixture, and the 500 and 19000 inches per inch per minute rates on a drop hammer.

The fracture ductility of hydrogen-charged steel at room temperature and normal testing strain rates ($\sim$0.05 inches per inch per minute) is a function of

electrolyzing time, dropping to a value that remains constant after a critical time (6)*. Under the conditions of this research the saturated loss in ductility occurred at approximately 30 minutes, see Fig. 4 and a sixty minute charging time was taken as standard for all subsequent tests.

After charging the steel with hydrogen, the surface was covered with blisters. These have been described by Seabrook, Grant and Carney (6). The original diameter of the specimen was not reduced by acid attack, even after ninety-one hours.

RESULTS

The ductility of both uncharged and charged specimens is given as a function of strain rate in Fig. 5, and as a function of temperature at four different strain rates in Fig. 6. These results are assembled into a three-dimensional graph in Fig. 7. It is seen that the locus of the minima in the ductility curves of the charged steels divides the ductility surface into two domains. At temperatures below the minima,

$$\frac{\partial \varepsilon}{\partial T})_{\dot{\varepsilon}} < 0 \quad \text{and} \quad \frac{\partial \varepsilon}{\partial \dot{\varepsilon}})_{T} > 0$$

(cf. for example, lines i and ii in Fig. 7); at temperatures above the minima

$$\frac{\partial \varepsilon}{\partial T})_{\dot{\varepsilon}} > 0 \quad \text{and} \quad \frac{\partial \varepsilon}{\partial \dot{\varepsilon}})_{T} > 0$$

(cf. for example, lines iii and iv in Fig. 7). These domains correspond to surfaces of types "a" and "d" respectively and the assembly corresponds to the prototype given in Fig. 3c.

- - - - - - -

* The hydrogen content of the steel continues to increase with charging time even after the ductility has leveled off to its saturated value (6).

DISCUSSION

Of the two types of ductility surfaces which characterize hydrogen embrittlement only the type "a" surface has been rationalized. Zapffe and Sims (9) and Zapffe (11) picture hydrogen embrittlement to result from the precipitation of hydrogen in "substructure disjunctions" or "voids" at pressures sufficient to force the metal assunder. Straining is presumed to enlarge the imperfections reducing the hydrogen pressure. Further precipitation of hydrogen is required to maintain or develop a disruptive pressure. With these premises, Zapffe proceeds to two conclusions:

"If the rate of strain is increased . . . . . until the rate of decrease in P_{H_2} exceeds the rate of restoration through further precipitation of H, the apparent embrittlement should decrease". This prediction states that

$$\left(\frac{\partial \varepsilon}{\partial \dot{\varepsilon}}\right)_T > 0$$

"The effect of temperature has an obviously similar relationship since the pressure of a gas phase likewise decreases with decreasing temperature. Thus there will be a critical temperature, also a critical rate of cooling, for any given set of conditions, such that the critical embrittlement pressure P_{H_2} is decreased more rapidly than it is replenished by precipitating H, and embrittlement is observed to decrease". This states that

$$\left(\frac{\partial \varepsilon}{\partial T}\right)_{\dot{\varepsilon}} < 0$$

These two conditions are those characterizing a ductility surface of type "a". Petch and Stables (4) extend Orowan's rationalization of the delayed fracture of glass to the case of hydrogen embrittlement. They point out that if hydrogen gas is adsorbed on the internal surface of microcracks, the critical stress for

extension of the crack in the Griffith relationship is lowered. "The extension of a crack under stress will take place in steps which occur when hydrogen solute atoms arrive at its edge in the course of diffusion". Since the proposed embrittling mechanism is diffusion-controlled, the authors point out that at high strain rates the metal should be ductile and adduced the data of Fig. 2c to support their conclusion. Again, this mechanism requires that

$$\left(\frac{\partial \varepsilon}{\partial \dot{\varepsilon}}\right)_T > 0$$

Although the authors made no statement regarding the effects of temperature it follows that if the arrival of the hydrogen to the microcracks is diffusion controlled, and since the diffusion rate decreases with decreasing temperature, then decreasing the test temperature at constant strain rate should increase the ductility, i.e.,

$$\left(\frac{\partial \varepsilon}{\partial T}\right)_{\dot{\varepsilon}} < 0$$

It is seen that the mechanism proposed by Petch and Stables, like Zapffe and Sims, corresponds to a ductility surface of type "a".

Both these mechanisms are variations on a theme: hydrogen embrittlement is presumed to depend upon the competition of two rates, the one being the rate of straining of the metal, the second being the rate of the embrittling controlling process (diffusion or precipitation) the latter rate being presumed to increase with increasing temperature. If the first rate predominates the metal is ductile, if the latter predominates the metal is brittle.

Surfaces of types b, c, and d can be rationalized by extension of the competitive rate hypothesis. If competition exists between the rate of straining and the rate of some process which renders the metal ductile the latter rate being presumed to

increase with increasing temperature, a surface of type "b" will result. The behavior of an overaging alloy on deformation illustrates this situation. Here overaging is a process that renders the alloy more ductile; its rate increases with increasing temperature. The ductility of such alloys as a function of strain rate and temperature yields a surface of type "b" (cf., for example, Fig. 10 of Ref. (13).

At constant strain rate, the ductility increases with increasing temperature because the rate of overaging increases with increasing temperature. At constant temperature, the ductility decreases with increasing strain rate, since the benign effect of the overaging process is outstripped.

Another example is the case of a hydrogen-charged steel in the process of degassing, since the degassification is a process rendering the metal ductile and its rate increases with increasing temperature (5)(6)(7)(9)(10). The increase in ductility of charged steel at temperatures above the minimum in Fig. 1a has been attributed to degassing (2), but such an explanation should not be indiscriminately put forward for such curves. The data in the present research represent a case in point, for the increase in ductility at temperatures above the minimum in Fig. 6, form a "d" surface and not the "b" surface that would be required, if degassing were the real explanation*.

If one wishes to extend the competitive rate hypothesis to describe surfaces of type "c" and "d" one must change the nature of temperature-sensitive process

- - - - - -

* The authors have no doubt that degassing is a factor in the hydrogen embrittlement of steels and suggest that a full characterization of the ductility surface of a charged steel would involve three domains instead of two, arranged in the manner of Fig. 8. Bastien and Azou's curve of Fig. 2b is quite probably a traverse across the type "a" and "b" surfaces of Fig. 8.

from one which increases with temperature to one that decreases with temperature. Such rates are found in super-cooled reactions such as the isothermal austenite-pearlite reaction at temperatures above the pearlite nose. If this process renders the metal ductile, a ductility surface of type "c" results. A type "d" surface results if the process is embrittling, since at constant strain rate an increase in temperature decreases the rate of the embrittling process and thus increases the ductility, i.e.,

$$\left(\frac{\partial \varepsilon}{\partial T}\right)_{\dot{\varepsilon}} > 0$$

while at constant temperature an increase in strain rate increases the ductility for the same reasons that it did in the case of the type "a" surface.

Undoubtedly there is significance in the fact that the two surfaces described by the present experimental results (types "a" and "d") if they are to be rationalized by competitive rate mechanisms, have one feature in common; in competition with the strain rate is a rate of an embrittling process irrespective of whether the rate increases or decreases with temperature. Since an embrittling process is common to both ductility surfaces, types "a" and "d", one suspects it is the same physical reaction in both cases.

A physical reaction which increases in rate with increasing temperature at low temperatures and decreases in rate with increasing temperature at high temperatures is not uncommon in the general realm of kinetics. The logarithm of the rate of such reactions when plotted against the reciprocal of the absolute temperature appears as "c" curves - exemplified by the rate of growth curve of pearlite, or scaling rate curves in surface oxidation studies.

The shape of these overall rate curves is usually the product of two main factors. The first is a driving force (such as free energy) which is zero at an

equilibrium temperature and which increases as reaction temperature is lowered from this point. The second is a mobility factor (such as diffusion or conductivity) which is generally of the form

$$D = D_o e^{-Q/RT}$$

such that the upper arm of the "c" curve approaches the equilibrium temperature asymptotically as the overall rate goes to zero (or log rate goes to minum infinity), and the lower arm of the "c" curve asymptotically approaches a straight line whose slope approximates the slope of the log mobility factor vs reciprocal absolute temperature curve, i.e , - Q/R as temperature goes to zero.

To obtain an approximation of the present overall rate curve, Fig. 9 plots the temperature (on a reciprocal absolute temperature scale) at which the ductility of the charged steels returns to the ductility curve of the uncharged steels (points "a" in Figs. 5 and 6) as a function of strain rate (on a log scale). One may assume that at these points there is some approximately fixed relationship between the strain rate and the rate of the embrittling reaction, so that the curve of Fig. 9 is an indication of the shape of the overall rate curve of the embrittling reaction.

There are two interesting reatures of the c-curve. The upper arm of the curve asymptotically approaches a limiting temperature, and by analogy with the A_1 temperature of a pearlite curve, or the oxide dissociation temperature in a scaling rate curve. This would represent an equilibrium temperature above which hydrogen has no embrittling effect on steels. The authors know of no change in the physical state of iron-hydrogen alloys in this temperature range which would account for this behavior.

The lower arm of the curve asymptotically approaches a sloping straight line. Again from the classical pattern of such curves one would infer that the slope of

the line should approximate the slope of the diffusion coefficient of hydrogen in alpha iron. The diffusion data (14) are meager and involve large extrapolations but a rough parallelism is nevertheless observed.

It must be inferred from Fig. 9 that if a competitive rate mechanism is to explain hydrogen embrittlement, then the rate, b, of the embrittling process must in some measure depend upon strain rate, for if

$$\varepsilon = f_2(\dot{\varepsilon}) - f_2(b)$$

then the minimum in the ductility curves would remain at a constant temperature which is obviously not the case in Fig. 9.

CONCLUSIONS

1. Hydrogen depresses the ductility of mild steel within certain ranges of temperature and strain rate only.
2. Within this brittle range, a plot of the ductility vs strain rate and temperature reveals two domains, one at low temperatures in which

$$\left(\frac{\partial \varepsilon}{\partial \dot{\varepsilon}}\right)_T > 0, \quad \left(\frac{\partial \varepsilon}{\partial T}\right)_{\dot{\varepsilon}} < 0$$

and another at high temperatures in which

$$\left(\frac{\partial \varepsilon}{\partial \dot{\varepsilon}}\right)_T > 0, \quad \left(\frac{\partial \varepsilon}{\partial T}\right)_{\dot{\varepsilon}} > 0$$

3. The first of these domains represents a behavior in accord with any theory - such as Zapffe and Sims' (9) or Petch and Stables (4) - which basically hypothesizes that the ductility of steels depends upon two competitive rates: the strain rate and a rate of the embrittling reaction which increases with increasing temperature, the steel being ductile if the former rate predominates, and brittle if the latter does.

4. The second of these domains is not explained by theories of this type, nor by the assumption that the steels are degassing (though the authors feel that a third domain due to degassification of the steel in which

$$\left(\frac{\partial \varepsilon}{\partial \dot{\varepsilon}}\right)_T < 0 \text{ and } \left(\frac{\partial \varepsilon}{\partial T}\right)_{\dot{\varepsilon}} > 0$$

does exist in certain temperature and strain rate ranges.

5. If the general proposition of two competitive rates is to be applied to the second of these domains, the rate of the embrittling reaction must <u>decrease</u> with increasing temperature.

6. An approximate curve of the logarithm of the rate of the embrittling reaction as a function of the reciprocal of the absolute temperature follows the classical pattern of rate curves of reactions that occur spontaneously below an equilibrium temperature, i.e., a "c" curve.

ACKNOWLEDGMENTS

This work was conducted in cooperation with the Office of Naval Research, U. S. Navy. The advice and help of Messrs. L. J. Ebert, I. Rozalsky and other members of the Metals Research Laboratory at Case Institute of Technology is greatly appreciated. Mr. T. S. Howald, Chase Brass and Copper Company, Inc. kindly loaned the platinum electrodes. The authors wish to thank the Westinghouse Electric Corporation for providing a Fellowship to one of us (J.T.B.).

BIBLIOGRAPHY

(1) National Bureau of Standard Pamphlet, Review of the Literature on Hydrogen Embrittlement of Steel, 1948.

(2) P. Bastien and P. Azou, "Effect of Hydrogen on the Deformation and Fracture of Iron and Steel in Simple Tension", Proceedings World Metallurgical Congress, American Society for Metals (1951), p. 535-552.

(3) P. Bastien and P. Azou, "Influence de l'amptitude et de la vitesse des deformations plastiques sur la segregation de la hydrogene dans le fer et les aciers", Comptes Rendues Vol. 232 (1951), p. 69-71.

(4) N. J. Petch and P. Stables, "Delayed Fracture of Metals under Static Load", Nature, Vol. 169 (1952), p. 842.

(5) C. E. Sims, G. A. Moore, D. W. Williams, "The Effect of Hydrogen on the Ductility of Cast Steels, "Transactions, American Institute of Mining and Metallurgical Engineers, Vol. 176 (1948), p. 283-308.

(6) J. B. Seabrook, N. J. Grant, and D. Carney, "Hydrogen Embrittlement of SAE 1020 Steel", Transactions, American Institute of Mining and Metallurgical Engineers, Vol. 188 (1950), p. 1317-1321.

(7) C. E. Sims, "Hydrogen Elimination by Aging", Transactions, American Institute of Mining and Metallurgical Engineers, Vol. 188 (1950), p. 1321.

(8) J. D. Hobson and C. Sykes, "Effect of Hydrogen on the Properties of Low Alloy Steels", Journal Iron and Steel Institute, Vol. 169 (1951), p. 209-220.

(9) C. A. Zapffe and C. E. Sims, "Hydrogen Embrittlement, Internal Stress and Defects in Steel", Transactions, American Institute of Mining and Metallurgical Engineers, Vol. 145 (1941), p. 225-259.

(10) S. H. Herres, "Practical Importance of Hydrogen in Metal-Arc Welding of Steel", Transactions American Society for Metals Vol. 39 (1947), p. 162-192.

(11) C. Zapffe, Discussion to Reference 10, Transactions American Society for Metals, Vol. 39 (1947), p. 190-191.

(12) J. D. Hobson and J. Hewitt, "The Effect of Hydrogen on the Tensile Properties of Steel", Journal Iron and Steel Institute, Vol. 173 (1953), p. 131-140.

(13) S. Epstein, "Aging of Iron and Steel" Metals Handbook, published by American Society for Metals, 1948 ed. p. 438-443.

(14) W. Geller and Tak-Ho Sun, "Einfluss von Legierungszusätzen auf die Wasserstoff diffusion im Eisen und Beitrag zum System Eisen-Wasserstoff" Archiv für das Eisenhüttenwesen, Vol. 21 (1950) p. 423-430.

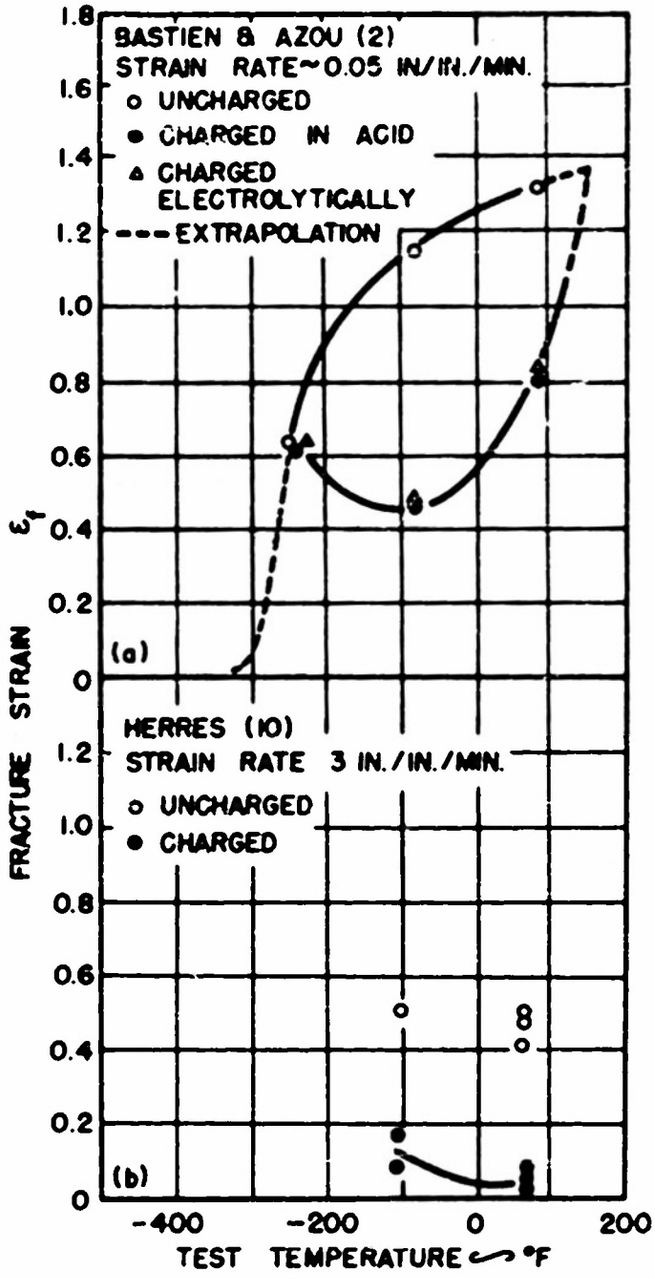

FIG. 1 : FRACTURE STRAIN AS A FUNCTION OF TESTING TEMPERATURE IN STEEL.

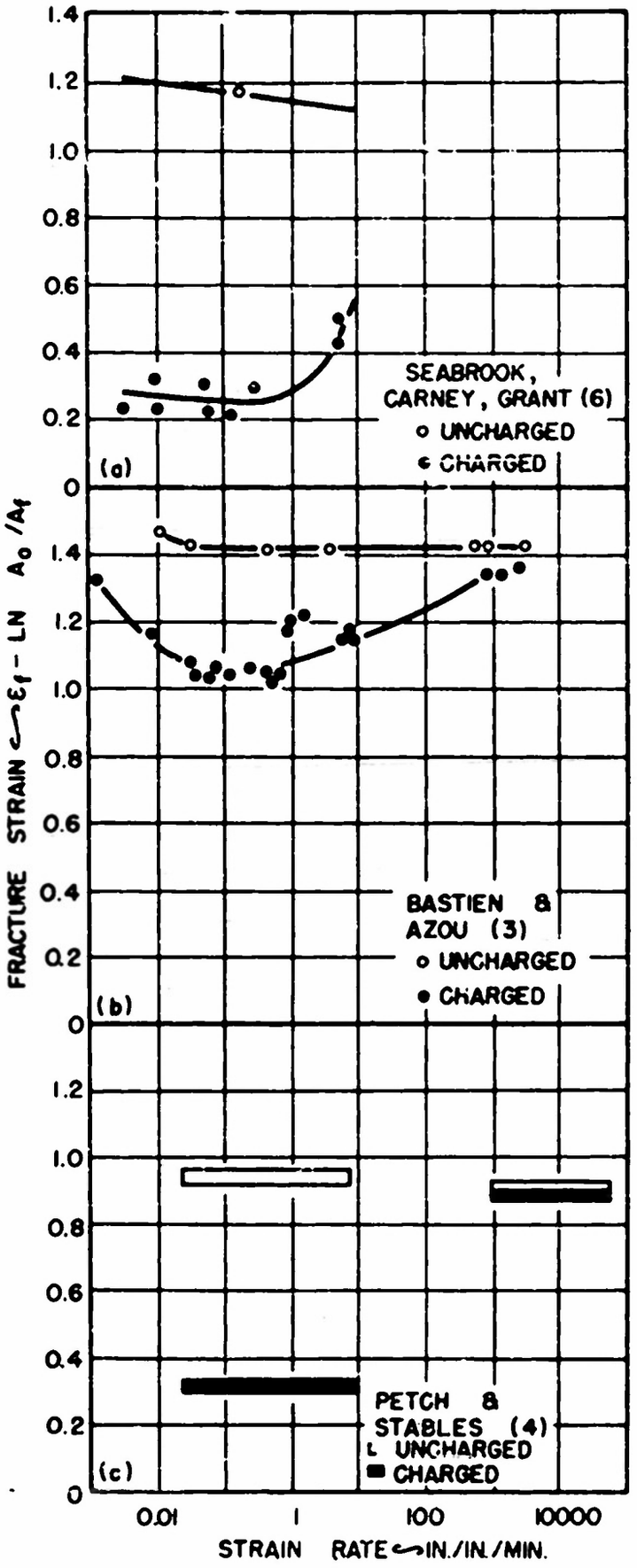

FIG. 2 : FRACTURE STRAIN AS A FUNCTION OF STRAIN RATE IN STEEL.

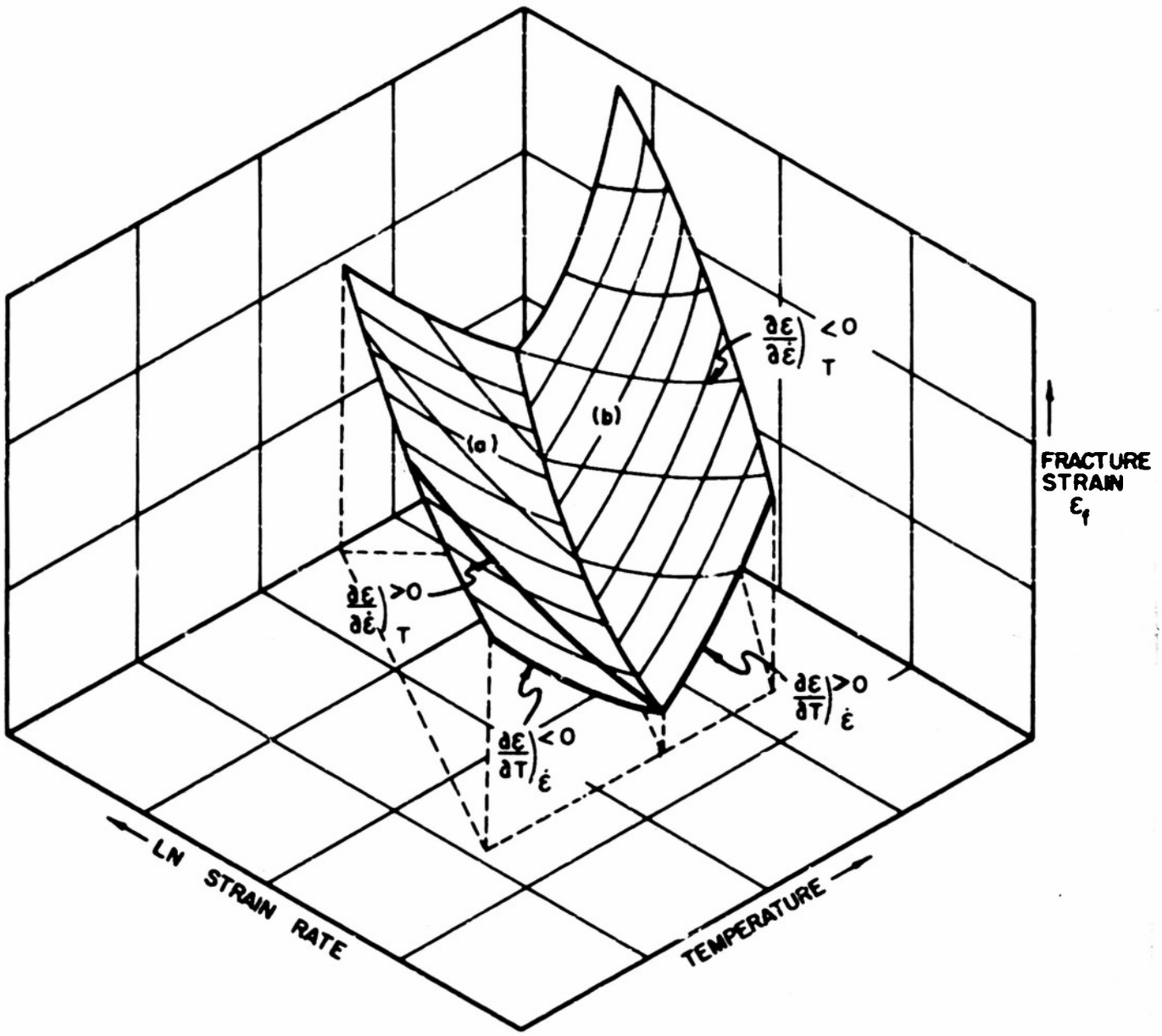

FIG. 3 – A: POSSIBLE CONSTRUCTION OF SHEETS TYPE "a" AND "b". DARK LINES INDICATE KNOWN TRAVERSES.

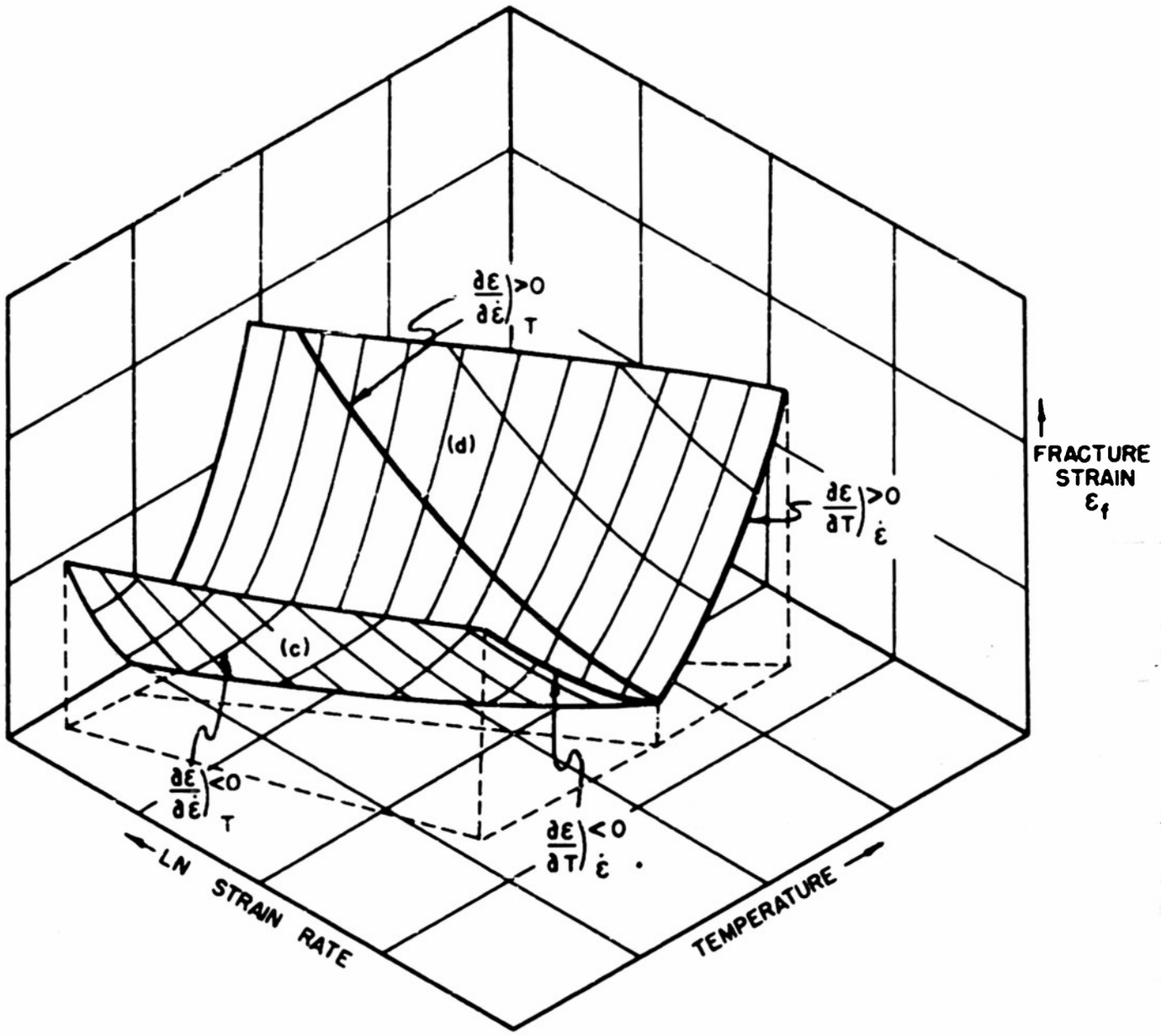

FIG. 3 – B : POSSIBLE CONSTRUCTION OF SHEETS TYPE "c" AND "d". DARK LINES INDICATE KNOWN TRAVERSES.

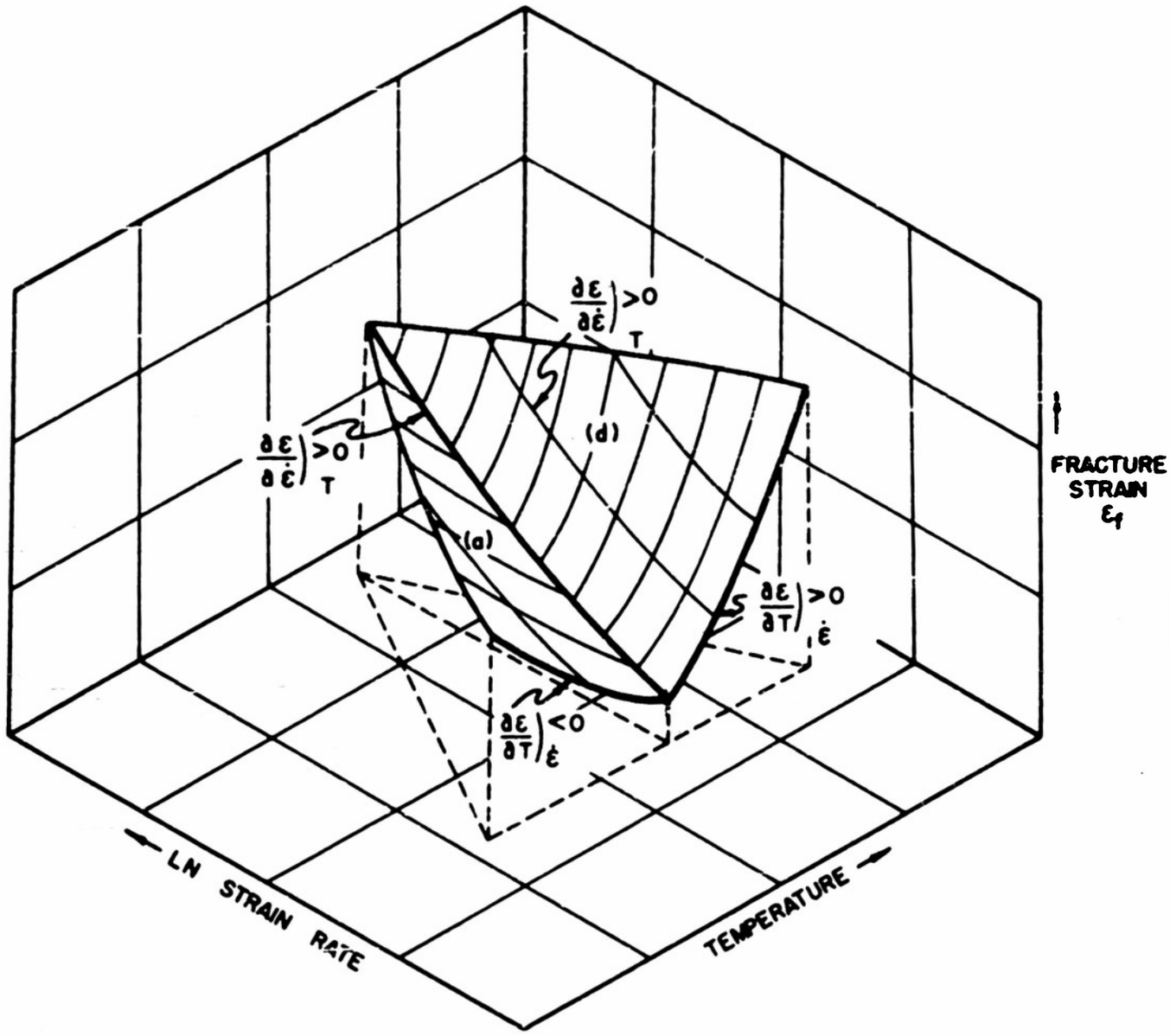

FIG. 3 – C : POSSIBLE CONSTRUCTION OF SHEETS TYPE "a" AND "d". DARK LINES INDICATE KNOWN TRAVERSES. THIS WAS ACTUALLY HOW HYDROGEN EMBRITTLEMENT WAS OBSERVED TO BEHAVE.

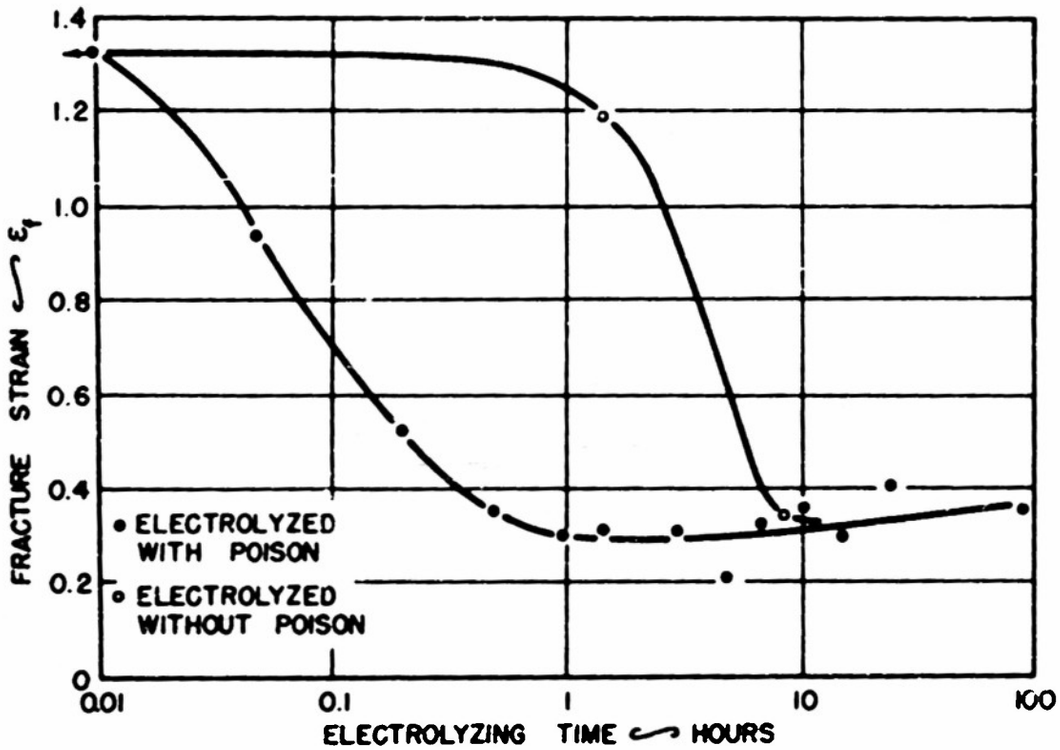

FIG. 4: FRACTURE STRAIN OF SPHEROIDIZED SAE 1020 STEEL AS A FUNCTION OF CHARGING TIME. NOTE ACCELERATING EFFECT OF POISON IN ELECTROLYTE ON CURVES AS WELL AS GENTLE UPSWING TO CURVES AT LONG TIMES.

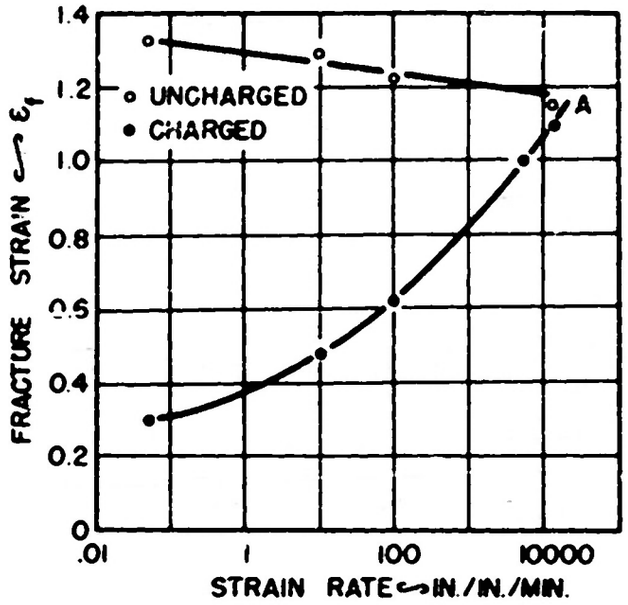

FIG. 5 : FRACTURE STRAIN AS A FUNCTION OF STRAIN RATE IN A CHARGED AND UNCHARGED SPHEROIDIZED SAE 1020 STEEL AT ROOM TEMPERATURE.

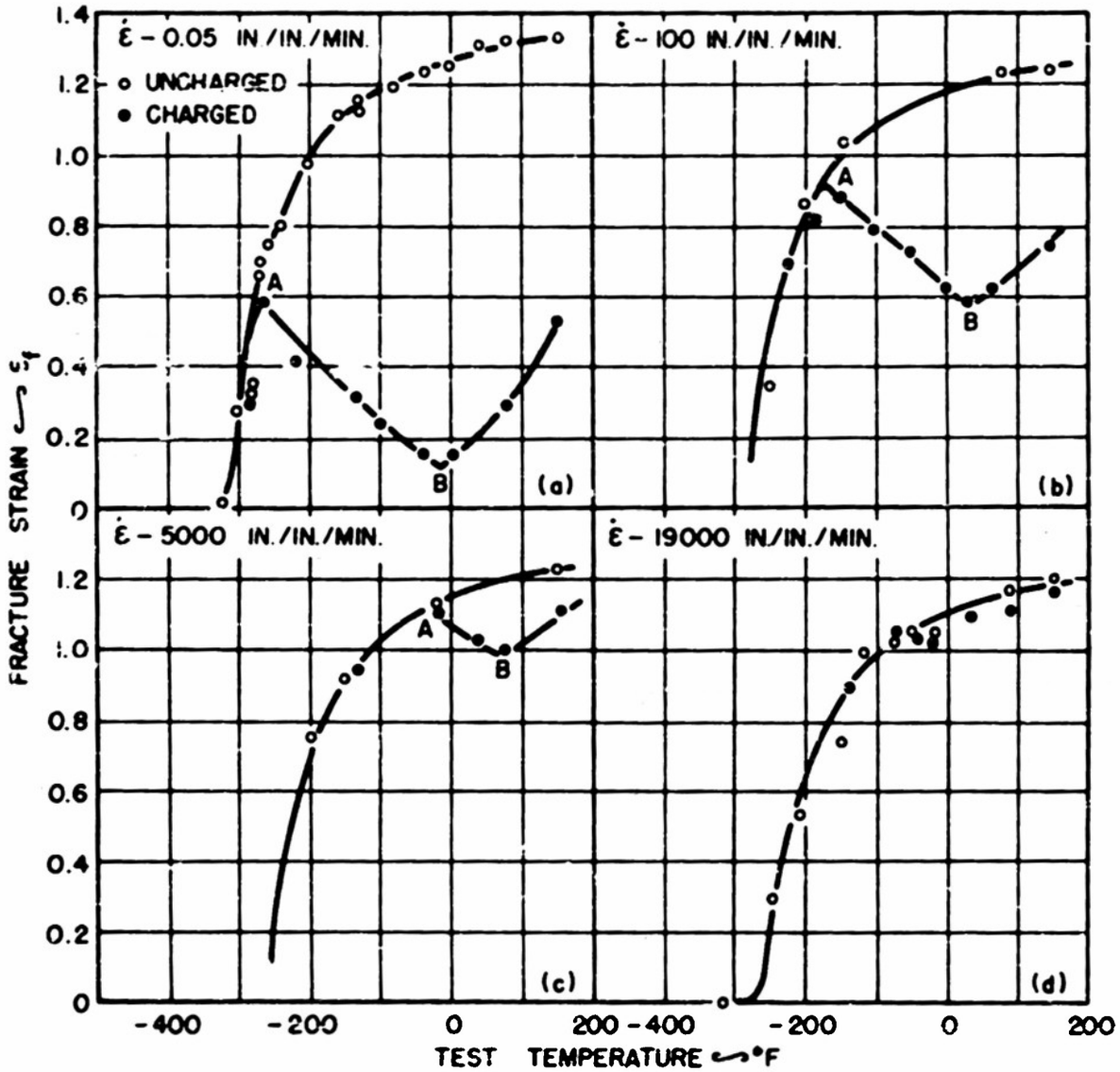

FIG. 6 : FRACTURE STRAIN OF SPHEROIDIZED 1020 STEEL WITH AND WITHOUT HYDROGEN EMBRITTLEMENT AS A FUNCTION OF TEST TEMPERATURE AND STRAIN RATE. THE TWO CURVES JOIN AT POINTS "A". A MINIMUM IN THE CURVES EXISTS AT POINTS "B".

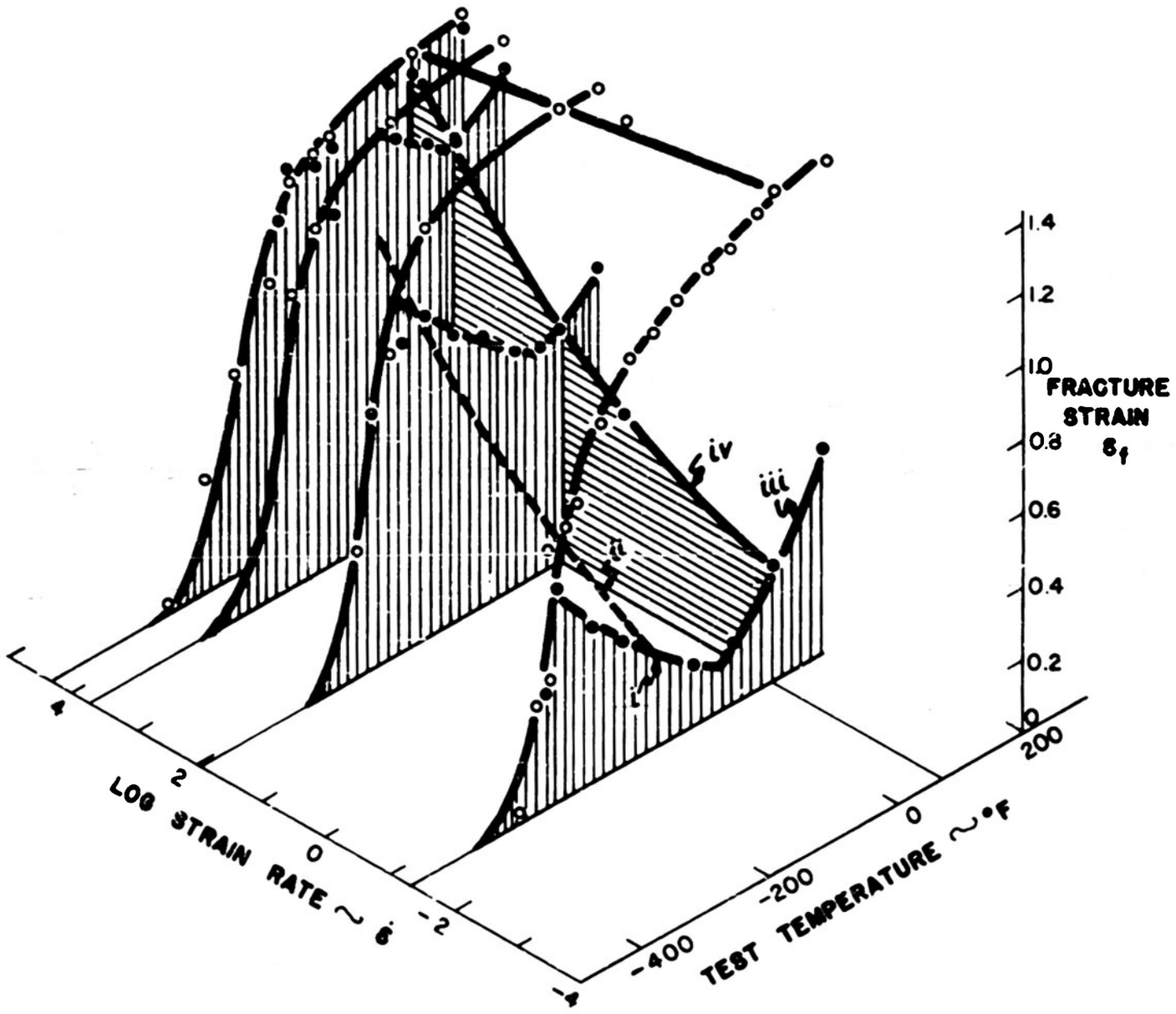

FIG. 7 : FRACTURE STRAIN OF SPHEROIDIZED SAE 1020 STEEL WITH & WITHOUT HYDROGEN EMBRITTLEMENT AS A FUNCTION OF TEMPERATURE & STRAIN RATE .

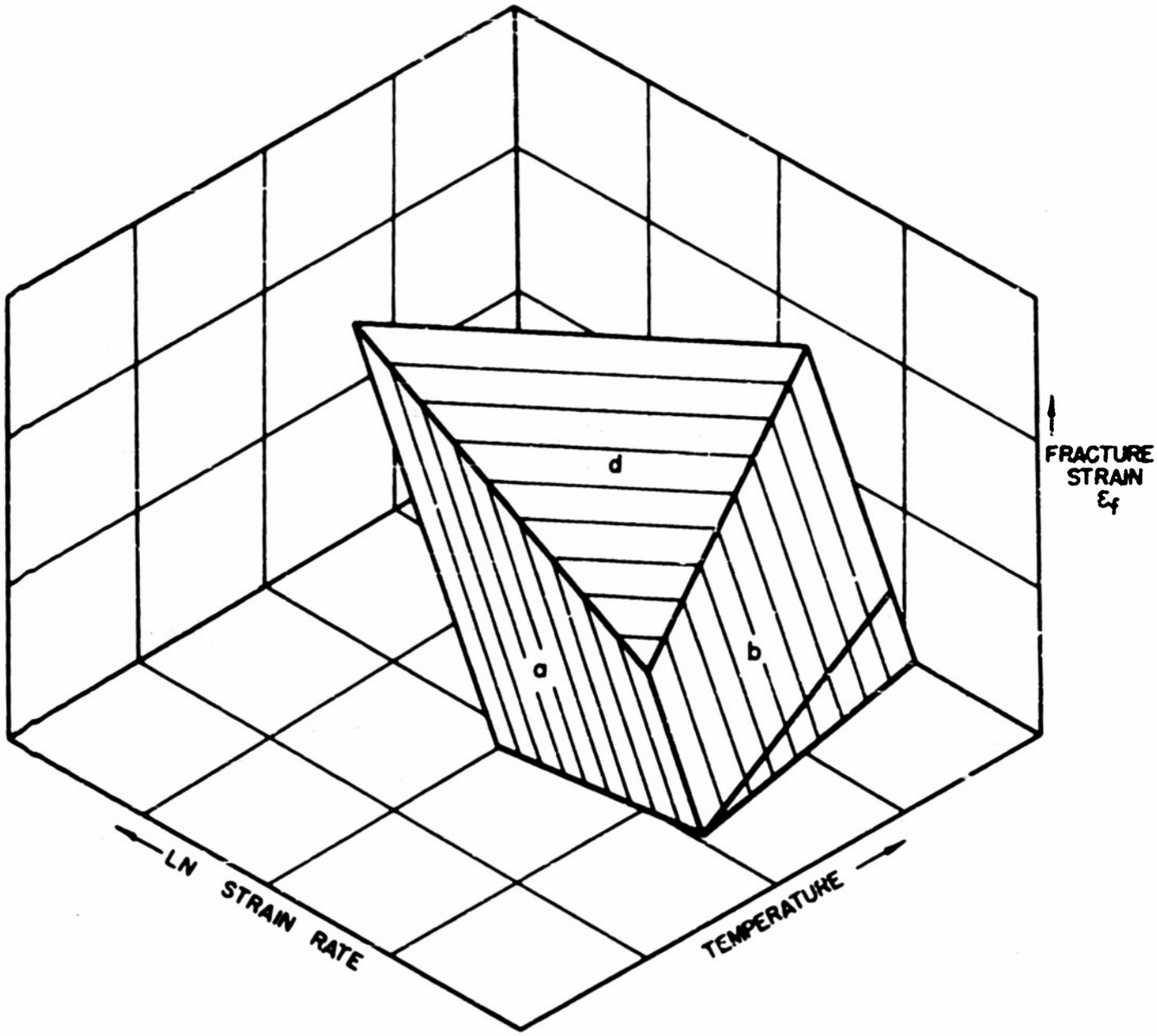

FIG. 8 : PROPOSED FULL CHARACTERIZATION OF HYDROGEN EMBRITTLEMENT.

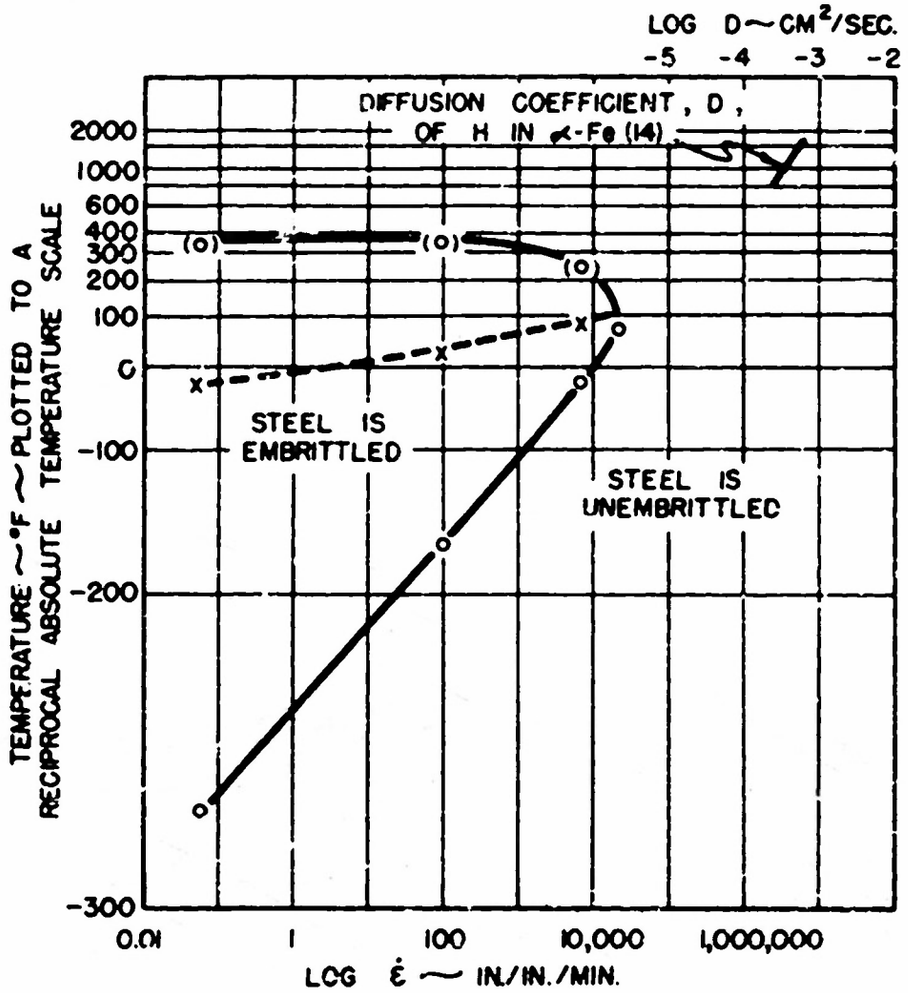

FIG. 9 : A PLOT OF TEMPERATURES AT WHICH DUCTILITY OF CHARGED STEELS RETURNS TO THE DUCTILITY CURVE OF UN-CHARGED STEELS AS A FUNCTION OF STRAIN RATE. THE CIRCLES PLOTTED HERE ARE THE POINTS "A" OF FIG. 6. POINTS IN PARENTHESES ARE EXTRAPOLATED FROM FIG. 6. THE CROSSES ARE THE POINTS "B" OF FIG 6, I.E. THE TEMPERATURES AND STRAIN RATES AT WHICH A MINIMUM IN THE DUCTILITY CURVES OCCURRED. THE DIFFUSION COEFFICIENT OF HYDROGEN IN ALPHA IRON IS PLOTTED TO THE UPPER SCALE.